

## NMR Characterization of Membrane Protein–Detergent Micelle Solutions by Use of Microcoil Equipment

Pawel Stanczak,<sup>†</sup> Reto Horst,<sup>†</sup> Pedro Serrano,<sup>†</sup> and Kurt Wüthrich<sup>\*†‡</sup>

Departments of Molecular Biology and Chemistry and Skaggs Institute for Chemical Biology,  
The Scripps Research Institute, 10550 North Torrey Pines Road, La Jolla, California 92037

Received September 15, 2009; E-mail: wuthrich@scripps.edu

**Abstract:** Using microcoil NMR technology, the uniformly <sup>2</sup>H,<sup>15</sup>N-labeled integral membrane protein OmpX, and the phosphocholine derivative detergent Fos-10 (*n*-decylphosphocholine), we investigated solutions of mixed protein–detergent micelles to determine the influence of the detergent concentration on the NMR spectra of the protein. In a first step, we identified key parameters that influence the composition of the micelle solutions, which resulted in a new protocol for the preparation of well-defined concentrated protein solutions. This led to the observation that high-quality 2D [<sup>15</sup>N,<sup>1</sup>H]-transverse relaxation-optimized spectroscopy (TROSY) spectra of OmpX reconstituted in mixed micelles with Fos-10 were obtained only in a limited range of detergent concentrations. Outside of this range from about 90–180 mM, we observed a significant decrease of the average peak intensity. Relaxation-optimized NMR measurements of the rotational and translational diffusion coefficients of the OmpX/Fos-10 mixed micelles, *D<sub>r</sub>* and *D<sub>t</sub>*, respectively, then showed that the stoichiometry and the effective hydrodynamic radius of the protein-containing micelles are not significantly affected by high Fos-10 concentrations and that the deterioration of NMR spectra is due to the increased viscosity at high detergent concentrations. The paper thus provides a basis for refined guidelines on the preparation of integral membrane proteins for structural studies.

### Introduction

Recent publications show that atomic-resolution structures of integral membrane proteins (IMPs) can be determined either by X-ray diffraction in single crystals<sup>1,2</sup> or by nuclear magnetic

resonance spectroscopy (NMR) in solution,<sup>3</sup> provided that diffracting crystals or structure-quality solutions of IMPs incorporated into detergent or lipid micelles are available. In apparent contrast, the Protein Data Bank (PDB)<sup>4</sup> contains only a small number of IMP structures when compared to soluble proteins, which is in no way correlated with the frequency at

<sup>†</sup> Department of Molecular Biology, The Scripps Research Institute.

<sup>‡</sup> Department of Chemistry and Skaggs Institute for Chemical Biology, The Scripps Research Institute.

- (1) (a) Faham, S.; Watanabe, A.; Besserer, G. M.; Cascio, D.; Specht, A.; Hirayama, B. A.; Wright, E. M.; Abramson, J. *Science* **2008**, *321*, 810–814. (b) Hilf, R. J. C.; Dutzler, R. *Nature* **2008**, *452*, 375–379. (c) Jaakola, V.-P.; Griffith, M. T.; Hanson, M. A.; Cherezov, V.; Chien, E. Y. T.; Lane, J. R.; Izerman, A. P.; Stevens, R. C. *Science* **2008**, *322*, 1211–1217. (d) Kadaba, N. S.; Kaiser, J. T.; Johnson, E.; Lee, A.; Rees, D. C. *Science* **2008**, *321*, 250–253. (e) Murakami, M.; Kouyama, T. *Nature* **2008**, *453*, 363–367. (f) Park, J. H.; Scheerer, P.; Hofmann, K. P.; Choe, H.-W.; Ernst, O. P. *Nature* **2008**, *454*, 183–187. (g) Remaut, H.; Tang, C.; Henderson, N. S.; Pinkner, J. S.; Wang, T.; Hultgren, S. J.; Thanassi, D. G.; Waksman, G.; Li, H. *Cell* **2008**, *133*, 640–652. (h) Scheerer, P.; Park, J. H.; Hildebrand, P. W.; Kim, Y. J.; Krausz, N.; Choe, H.-W.; Hofmann, K. P.; Ernst, O. P. *Nature* **2008**, *455*. (i) Stouffer, A. L.; Acharya, R.; Salom, D.; Levine, A. S.; Di Costanzo, L.; Soto, C. S.; Tereshko, V.; Nanda, V.; Stayrook, S.; DeGrado, W. F. *Nature* **2008**, *451*, 596–599. (j) Tsukazaki, T.; Mori, H.; Fukai, S.; Ishitani, R.; Mori, T.; Dohmae, N.; Perederina, A.; Sugita, Y.; Vassilyev, D. G.; Ito, K.; Nureki, O. *Nature* **2008**, *455*, 988–991. (k) Wang, W.; Black, S. S.; Edwards, M. D.; Miller, S.; Morrison, E. L.; Bartlett, W.; Dong, C.; Naismith, J. H.; Booth, I. R. *Science* **2008**, *321*, 1179–1183. (l) Warne, T.; Serrano-Vega, M. J.; Baker, J. G.; Moukhametzianov, R.; Edwards, P. C.; Henderson, R.; Leslie, A. G. W.; Tate, C. G.; Schertler, G. F. X. *Nature* **2008**, *454*, 486–491. (m) Weyand, S.; et al. *Science* **2008**, *322*, 709–713. (n) Zimmer, J.; Nam, Y.; Rapoport, T. A. *Nature* **2008**, *455*, 936–943. (o) Gerber, S.; Comellas-Bigler, M.; Goetz, B. A.; Locher, K. P. *Science* **2008**, *321*, 246–250. (p) Singh, S. K.; Piscitelli, C. L.; Yamashita, A.; Gouaux, E. *Science* **2008**, *322*, 1655–1661. (q) Shinoda, T.; Ogawa, H.; Cornelius, F.; Toyoshima, C. *Nature* **2009**, *459*, 446–450. (r) Aller, S. G.; Yu, J.; Ward, A.; Weng, Y.; Chittaboina, S.;

Zhuo, R.; Harrell, P. M.; Trinh, Y. T.; Zhang, Q.; Urbatsch, I. L.; Chang, G. *Science* **2009**, *323*, 1718–1722. (s) Shaffer, P. L.; Goehring, A.; Shankaranarayanan, A.; Gouaux, E. *Science* **2009**, *325*, 1010–1014. (t) Gao, X.; Lu, F.; Zhou, L.; Dang, S.; Sun, L.; Li, X.; Wang, J.; Shi, Y. *Science* **2009**, *324*, 1565–1568. (u) Fang, Y.; Jayaram, H.; Shane, T.; Kolmakova-Partensky, L.; Wu, F.; Williams, C.; Xiong, Y.; Miller, C. *Nature* **2009**, *460*, 1040–1043. (v) Bocquet, N.; Nury, H.; Baaden, M.; Le Poupon, C.; Changeux, J.-P.; Delarue, M.; Corringer, P.-J. *Nature* **2009**, *457*, 111–114. (w) Gonzales, E. B.; Kawate, T.; Gouaux, E. *Nature* **2009**, *460*, 599–604. (x) Hearn, E. M.; Patel, D. R.; Lepore, B. W.; Indic, M.; van den Berg, B. *Nature* **2009**, *458*, 367–370. (y) Hilf, R. J. C.; Dutzler, R. *Nature* **2009**, *457*, 115–118.

- (2) (a) Kawate, T.; Michel, J. C.; Birdsong, W. T.; Gouaux, E. *Nature* **2009**, *460*, 592–598. (b) Maeda, S.; Nakagawa, S.; Suga, M.; Yamashita, E.; Oshima, A.; Fujiyoshi, Y.; Tsukihara, T. *Nature* **2009**, *458*, 597–602. (c) Mueller, M.; Grauschopf, U.; Maier, T.; Glockshuber, R.; Ban, N. *Nature* **2009**, *459*, 726–730. (d) Ressler, S.; Terwisscha van Scheltinga, A. C.; Vonrhein, C.; Ott, V.; Ziegler, C. *Nature* **2009**, *458*, 47–52. (e) Stein, A.; Weber, G.; Wahl, M. C.; Jahn, R. *Nature* **2009**, *460*, 525–528.
- (3) (a) Hiller, S.; Garces, R. G.; Malia, T. J.; Orekhov, V. Y.; Colombini, M.; Wagner, G. *Science* **2008**, *321*, 1206–1210. (b) Van Horn, W. D.; Kim, H. J.; Ellis, C. D.; Hadziselimovic, A.; Sulistijo, E. S.; Karra, M. D.; Tian, C.; Sonnichsen, F. D.; Sanders, C. R. *Science* **2009**, *324*, 1726–1729. (c) Schnell, J. R.; Chou, J. J. *Nature* **2008**, *451*, 591–595.
- (4) (a) Berman, H. M.; Westbrook, J.; Feng, Z.; Gilliland, G.; Bhat, T. N.; Weissig, H.; Shindyalov, I. N.; Bourne, P. E. *Nucleic Acids Res.* **2000**, *28*, 235–242. (b) A total of 203 membrane protein structures were deposited in the PDB up to 9/9/2009.

which the two classes of proteins are represented in the genomes of higher or lower organisms.<sup>5</sup> The PDB thus documents a stringent bottleneck that slows down the structural biology of membrane proteins, that is, the preparation of diffracting crystals or concentrated solutions of stable-isotope-labeled IMPs for high-resolution structure determination. The present paper describes systematic studies of size and composition of mixed IMP–detergent micelles in solution under variable conditions of detergent concentration, protein concentration, and experimental setup. The results thus obtained should contribute to developing improved protocols for IMP preparation for either NMR or X-ray diffraction studies. The present experiments further bear on the solvation of IMP structures in aqueous solutions of mixed micelles with detergents, which may in turn also provide new insights into the behavior of IMPs in cocrystals with detergents and lipids, which are often obtained from such solutions.

The present study follows up on previous work by different authors, which showed that the physicochemical properties of the detergent, in particular critical micelle concentration (cmc), aggregation number, and hydrophobicity and charge, can play a key role in a successful sample preparation and may strongly influence the quality of the NMR spectra recorded with solutions of micelle-solubilized IMPs.<sup>6–8</sup> From the available data it is also readily apparent that appropriate choice of the detergent concentration is generally considered to be a key to successful solubilization and reconstitution of IMPs. For NMR structure determinations, detergent concentrations in the range from 200 to 600 mM have been reported,<sup>3,9</sup> and it has also been suggested that the detergent micelle concentration should be much higher than the protein concentration,<sup>8</sup> where the micelle concentration is estimated as  $(\text{total detergent concentration} - \text{cmc})/N_a$ , where  $N_a$  is the aggregation number, which indicates the number of detergent molecules contained in a micelle.<sup>6</sup>

Using a previously presented microscale protocol for obtaining high-quality NMR data for the  $\beta$ -barrel outer membrane protein X (OmpX)<sup>10</sup> as a starting platform, we optimized the procedure to obtain improved yields of OmpX under controlled solution conditions. Thereby, it was of special concern that the detergent content in the concentrated protein solutions needed for NMR measurements or for crystallization attempts may greatly vary depending on the equipment and the conditions used for the concentration steps and cannot in a straightforward

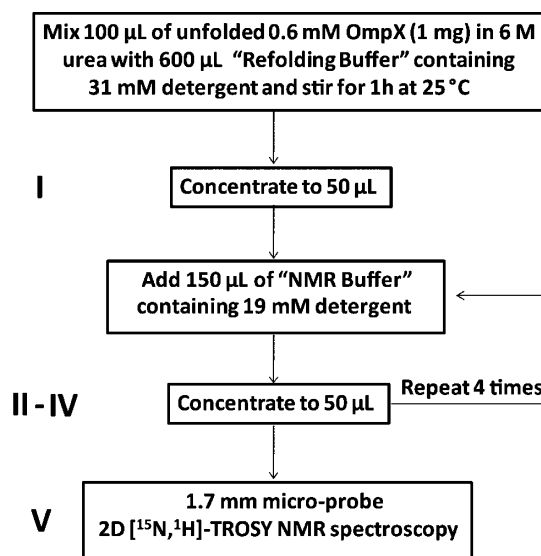


**Figure 1.** Standard protocol used for microscale preparation of NMR samples of OmpX reconstituted with the detergent Fos-10. In the first step, urea-unfolded OmpX is reconstituted in Fos-10 micelles. In the second step, the volume of the solution of mixed micelles in the refolding buffer is reduced to 50  $\mu\text{L}$ , by use of centrifugal concentration devices with membranes of MWCO = 10 kDa. In each of four subsequent steps the concentrated protein solution is diluted with a 3-fold excess of NMR buffer, and with the aforementioned centrifugal device the sample volume is again reduced to 50  $\mu\text{L}$ . Protein and detergent concentrations, MWCO of the centrifugal device, reaction temperature, reaction times, and repeats of individual steps indicated in the figure are the result of a procedure optimization described in the first part of this paper (buffers are described in the Materials and Methods section). They are different from the conditions used previously with the same overall setup.<sup>10</sup> The optimization was pursued by monitoring the detergent and protein concentrations in solutions I–V. Solution V corresponds to the final sample, for which a 2D [<sup>15</sup>N,<sup>1</sup>H]-correlation NMR experiment was also recorded (see Materials and Methods).

way be monitored via the detergent concentration in the buffer solutions used. In this paper we tightly monitor the detergent concentration and the quality of NMR spectra obtained at various stages of the OmpX preparation procedure (Figure 1) and thus derive rules on how the detergent concentration in the final NMR sample is affected by the concentration of detergent in the NMR buffer, the type of centrifugal device used, the centrifugal device molecular weight cutoff (MWCO), temperature, and protein concentration. Since this project required the screening of a large series of samples containing the uniformly <sup>2</sup>H,<sup>15</sup>N-labeled IMP, the use of microscale NMR spectroscopy to monitor the composition of the buffer and the quality of the protein–detergent micelles during the sample preparation was key to making this study economically viable.

The aforementioned preparative and analytical work sets the stage for investigations on the influence of various solution parameters on the size of mixed micelles in solution, the quality of the high-resolution NMR spectra obtained, and other parameters. This part of the project is pursued with a suite of NMR experiments for investigations of the rotational and translational diffusion of biological macromolecules and macromolecular assemblies.

## Materials and Methods

Unlabeled and uniformly [<sup>2</sup>H,<sup>15</sup>N]-labeled OmpX was expressed as inclusion bodies in *Escherichia coli* and purified to yield a solution of the unfolded protein in 6 M urea.<sup>10</sup> The detergent selected for OmpX reconstitution in this study is the phosphocholine

- (5) Wallin, E.; von Heijne, G. *Protein Sci.* **1998**, *7*, 1029–1038.  
 (6) McDonnell, P. A.; Opella, S. J. *J. Magn. Reson.* **1993**, *B102*, 120–125.  
 (7) Krueger-Koplin, R. D.; Sorgen, P. L.; Krueger-Koplin, S. T.; Rivera-Torres, I. O.; Cahill, S. M.; Grinius, L.; Krulwicz, T. A.; Grivin, M. E. *J. Biomol. NMR* **2004**, *17*, 43–57.  
 (8) (a) Marassi, F. M.; Opella, S. J. *Curr. Opin. Struct. Biol.* **1998**, *8*, 640–648. (b) Sanders, R. S.; Oxenoid, K. *Biochim. Biophys. Acta* **2000**, *1508*, 129–145. (c) Sanders, R. S.; Sonnichsen, F. *Magn. Reson. Chem.* **2006**, *S24–S40*.  
 (9) (a) Arora, A.; Abildgaard, F.; Bushweller, J. H.; Tamm, L. K. *Nature* **2001**, *8*, 334–338. (b) Hwang, P. M.; Choy, W.; Lo, E. I.; Chen, L.; Forman-Kay, J. D.; Raetz, C. R. H.; Prive, G. G.; Bishop, R. E.; Kay, L. E. *Proc. Natl. Acad. Sci. U.S.A.* **2002**, *99*, 13560–13565. (c) Fernandez, C.; Hilty, C.; Wider, G.; Güntert, P.; Wüthrich, K. *J. Mol. Biol.* **2004**, *336*, 1211–1221. (d) Oxenoid, K.; Chou, J. J. *Proc. Natl. Acad. Sci. U.S.A.* **2005**, *102*, 10870–10875. (e) Teriete, P.; Franzin, C. M.; Choi, J.; Marassi, F. M. *Biochemistry* **2007**, *46*, 6774. (f) Liang, B.; Tamm, L. K. *Proc. Natl. Acad. Sci. U.S.A.* **2007**, *104*, 16140–16145. (g) Zhou, Y.; Cierpicki, T.; Jimenez, R. H. F.; Lukasik, S. M.; Ellena, J. F.; Cafiso, D. S.; Kadokura, H.; Beckwith, J.; Bushweller, J. H. *Mol. Cell* **2008**, *31*, 896–908.  
 (10) Zhang, Q.; Horst, R.; Geralt, M.; Ma, X.; Hong, W.; Finn, M. G.; Stevens, R. C.; Wüthrich, K. *J. Am. Chem. Soc.* **2008**, *130*, 7357–7363.

derivative *n*-decylphosphocholine (Fos-10; Anatrace, Maumee, OH), which is a representative of a family of detergents that have previously been shown to yield high-quality NMR spectra of the protein OmpX<sup>10</sup> and other  $\beta$ -barrel membrane proteins (unpublished data).

**Reconstitution of OmpX in Fos-10 Micelles for NMR Spectroscopy.** The protocol for preparation of NMR samples containing OmpX in mixed micelles with Fos-10 starts with the purified protein in 6 M urea solution. The protein is reconstituted by addition of an excess of “refolding buffer” containing 20 mM Tris-HCl at pH 8.0, 5 mM ethylenediaminetetraacetic acid (EDTA), 600 mM L-Arg, and the detergent and by stirring of the resulting new solution (Figure 1). Next, the solution of the refolded protein is concentrated to 50  $\mu$ L by use of centrifugal concentration devices with a given molecular weight cutoff (MWCO). This concentrated solution is then repeatedly diluted with “NMR buffer” containing 5 mM sodium phosphate at pH 6.8, 10 mM NaCl, 0.3% NaN<sub>3</sub>, and detergent, and the volume is again reduced to 50  $\mu$ L by centrifugation. After a sufficient number of dilution/concentration cycles for complete replacement of the refolding buffer with NMR buffer, a sample for microcoil NMR spectroscopy is obtained. The “standard conditions” indicated in Figure 1 were selected on the basis of optimization of this procedure in the present paper and differ from the previously reported conditions used with the same setup.<sup>10</sup> The final NMR sample contained 45  $\mu$ L of the concentrated OmpX solution supplemented with 5  $\mu$ L of D<sub>2</sub>O and 1  $\mu$ L of a 100 mM solution of 2,2-dimethyl-2-silapentane-3,3,4,4,5,5-*d*<sub>6</sub>-5-sulfonate sodium salt (DSS), which was added as an internal reference for the <sup>1</sup>H chemical shifts as well as the peak integrals in the 1D <sup>1</sup>H NMR spectra.

**NMR Spectroscopy.** All NMR experiments were recorded at 25 °C on a Bruker DRX-700 spectrometer equipped with a 1.7 mm TXI microcoil probe head (Bruker, Billerica, MA). One-dimensional <sup>1</sup>H NMR spectra were collected with the following parameters: complex data size = 16K, acquisition time = 1.38 s; number of scans = 128, sweep width = 11 900 Hz. Two-dimensional [<sup>15</sup>N,<sup>1</sup>H]-transverse relaxation-optimized spectroscopy (TROSY) correlation experiments were recorded as described previously,<sup>10,11</sup> and details of the TROSY parameter settings are given in the legend of Figure 4. The NMR data were processed by use of the software TOPSPIN 1.3 (Bruker). The analysis of the [<sup>15</sup>N,<sup>1</sup>H]-TROSY correlation spectra was performed with XEASY,<sup>12</sup> and the TRACT and REST data (see below) were analyzed by use of in-house TOPSPIN macros in combination with the program XMGRACE (<http://plasma-gate.weizmann.ac.il>).

**Monitoring the Sample Composition at Discrete Points of the Preparation Protocol.** The detergent concentration was determined in solutions I–V (Figure 1) by comparing the integral of the Fos-10 trimethylamino signal at 3.22 ppm in the 1D <sup>1</sup>H NMR spectra with the DSS signal intensity at 0 ppm (Figure 2). To monitor the quality of the NMR spectra obtained in the different experiments, 2D [<sup>15</sup>N,<sup>1</sup>H]-TROSY correlation spectra were recorded in solution V.

The OmpX concentration was checked by UV spectroscopy, as follows: 1  $\mu$ L of the concentrated solution of refolded OmpX was diluted 25-fold in 20 mM Tris-HCl at pH 8.5 that contained 6 M urea, and this solution was then stirred at 25 °C for 12 h to ensure complete unfolding of the protein. Then the absorption at 280 nm was measured with a nanodrop instrument (ND-1000 spectrophotometer).

**NMR Characterization of the OmpX/Fos-10 Mixed Micelles.** The effective rotational correlation time of the OmpX/Fos-10 micelles,  $\tau_c$ , was determined by the TRACT experiment.<sup>13</sup> A total of 128 relaxation delays ranging from 1 to 129 ms were used, with 512 scans per relaxation delay. The relaxation rates  $R_\alpha$  and  $R_\beta$  were obtained by fitting the integrals over all the peaks

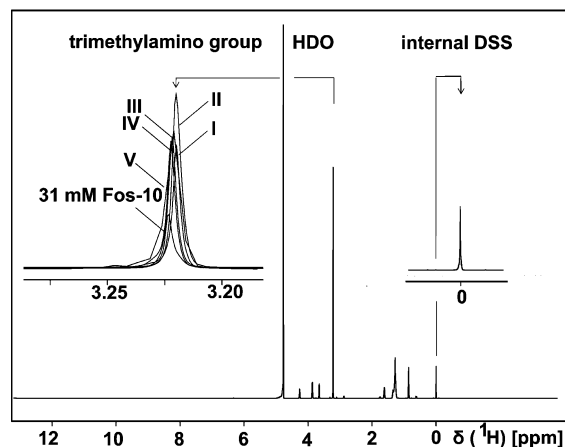


**Figure 2.** One-dimensional <sup>1</sup>H NMR spectra used to monitor the Fos-10 concentration of solutions I–V identified in Figure 1 for the following experiment: detergent concentration in NMR buffer = 19 mM, OmpX concentration = 1.0 mM. The spectra were recorded at 700 MHz, by use of a 1.7 mm microprobe. The singlet resonance at 3.22 ppm corresponds to the trimethylamino group of Fos-10. The DSS signal at 0 ppm was used as an internal reference for both the <sup>1</sup>H chemical shifts and the peak integrals in the 1D <sup>1</sup>H NMR spectra. Expanded plots of the Fos-10 trimethylamino signal, which shows small chemical shift differences in the various buffer compositions, and the DSS signal in solutions I–V are superimposed in the two insets, as indicated in the figure.

between 10.0 and 7.0 ppm to a one-parameter exponential decay and were then used to calculate  $\tau_c$ .<sup>13</sup>

The translational diffusion constant,  $D_t$ , was measured by a relaxation-optimized <sup>15</sup>N-edited stimulated echo (STE) experiment (REST).<sup>14</sup> A series of 16 diffusion-weighted one-dimensional spectra were recorded in a two-dimensional manner, using a pair of gradient pulses of 4.5 ms duration separated by 100 ms, with gradient strengths ranging from 3 to 55 G cm<sup>-1</sup>. The pulsed field gradient strengths were calibrated with the residual <sup>1</sup>H signal in 99.9% D<sub>2</sub>O, by use of a self-diffusion coefficient for HDO at 25 °C of  $(1.902 \pm 0.002) \times 10^{-9}$  m<sup>2</sup> s<sup>-1</sup>.<sup>15</sup>  $D_t$  was then obtained by fitting the signal volume with eq 1:

$$I = I_0 \exp\{-\gamma^2 G^2 \delta^2 (\Delta - \delta/3) D_t\} \quad (1)$$

$\gamma$  is the <sup>1</sup>H gyromagnetic ratio, and  $G$ ,  $\delta$ , and  $\Delta$  are the amplitude, duration, and separation of the gradient pulses, respectively. To determine the translational diffusion constant of OmpX, the integral over the NMR signals in the interval 7.0–10.0 ppm was measured to obtain values for  $I$  and  $I_0$ .

**Analysis of the Rotational and Translational Diffusion Constants.** We use the Stokes–Einstein (SE) model to describe the dependence of rotational and translational diffusion constants on solution viscosity ( $\eta$ ) and hydrodynamic radius (“Stokes radius”,  $R_h$ ) for spherical, noninteracting particles:

$$D_t = k_B T / (6\pi\eta R_h) \quad (2)$$

$$D_r = k_B T / (8\pi\eta R_h^3) \quad (3)$$

where  $k_B$  is the Boltzmann constant,  $T$  is the absolute temperature, and  $D_t$  and  $D_r$  are the translational and rotational diffusion constants, respectively.  $D_r$  is related to the effective rotational correlation time,  $\tau_c$ , by

(12) Bartels, C.; Xia, T.; Billeter, M.; Güntert, P.; Wüthrich, K. *J. Biomol. NMR* **1995**, *6*, 1–10.

(13) Lee, D.; Hilty, C.; Wider, G.; Wüthrich, K. *J. Magn. Reson.* **2006**, *178*, 72–76.

(14) Horst, R.; Wüthrich, K. Manuscript in preparation.

(15) Mills, R. *J. Phys. Chem.* **1973**, *77*, 685–688.

(11) Pervushin, K.; Riek, R.; Wider, G.; Wüthrich, K. *Proc. Natl. Acad. Sci. U.S.A.* **1997**, *94*, 12366–12377.

$$D_r = 1/6\tau_c \quad (4)$$

Equations 2 and 3 lead to an expression for the effective hydrodynamic radius of an equivalent sphere,  $R_h$ , which is independent of  $\eta$ :

$$R_h = \sqrt{3D_r/4D_r} \quad (5)$$

The experimental translational and rotational diffusion constants can thus be used to determine  $R_h$  of macromolecular assemblies, such as protein–detergent mixed micelles, within the validity of the Stokes–Einstein model for an equivalent sphere representing the macromolecular structure.

**Computational Evaluation of the Micelle Radius  $R_m$ .** A hypothetical value for the radius of OmpX/Fos-10 mixed micelles was estimated for the situation that the Fos-10 molecules in the solution would either be bound to mixed micelles or monomeric, that is, with the assumption that there would be no empty Fos-10 micelles in the solution. For this situation, the volume of the mixed micelles,  $V_m$ , was computed as

$$V_m = V_{\text{OmpX}} + V_{\text{Fos10}}(c_{\text{Fos10}} - \text{cmc}_{\text{Fos10}})/c_{\text{OmpX}} = V_{\text{OmpX}} + \frac{V_{\text{Fos10}}N_a}{c_{\text{OmpX}}} \quad (6)$$

where  $V_{\text{OmpX}}$  is the volume of the protein ( $18.2 \times 10^3 \text{ \AA}^3$ ),<sup>16</sup>  $V_{\text{Fos10}}$  is the Fos-10 monomer volume ( $494 \text{ \AA}^3$ ),<sup>17</sup>  $N_a$  is the aggregation number,  $\text{cmc}_{\text{Fos10}} = 10.8 \text{ mM}$  is the critical micelle concentration for Fos-10, and  $c_{\text{Fos10}}$  and  $c_{\text{OmpX}}$  are the experimentally determined total concentrations of Fos-10 and OmpX in the solution in molar units. If the mixed micelles are represented by an equivalent sphere, the radius of this sphere,  $R_m$ , is given by

$$R_m = \sqrt[3]{3V_m/4\pi} \quad (7)$$

The  $R_m$  value obtained with eq 7 is a lower boundary for the effective hydrodynamic radius  $R_h$ , since eqs 6 and 7 do not take into account the hydration shell of the mixed micelle, and deviations from spherical shape always lead to larger effective  $R_h$  values for the equivalent sphere.<sup>18</sup>

## Results and Discussion

It has been well established that the nature and concentration of the detergents used for integral membrane protein (IMP) solubilization and reconstitution in aqueous solvents are critical factors in successful IMP preparations for structural biology. However, although it is straightforward to establish well-defined detergent concentrations in the starting buffer solutions, variation of the detergent concentration during dialysis and sample concentration results in uncertainty about the composition of the highly concentrated protein solutions needed either for NMR spectroscopy or for crystallization trials.<sup>19</sup> In the first part of the present project, we therefore introduce an experimental setup that enables us to monitor the amount of detergent present at discrete stages of the sample preparation and in the final, concentrated protein solution. We then use this procedure to investigate the influence of different parameters on the final sample composition, such as the buffers used, the protein concentration, the type of membrane used in the centrifugal

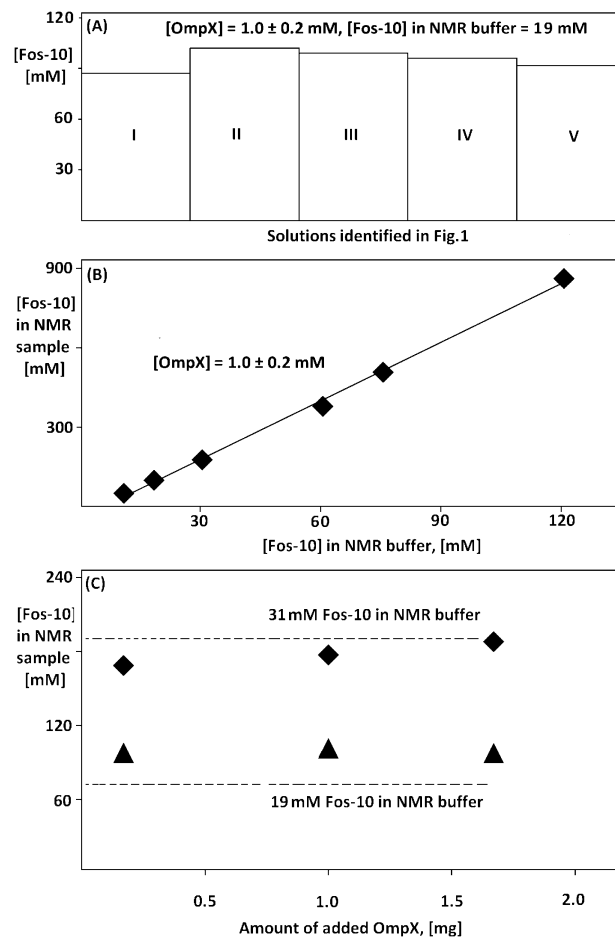


**Figure 3.** Up-concentration of Fos-10 during OmpX refolding monitored by microscale 1D  $^1\text{H}$  NMR. (A) Histogram presentation of the detergent concentrations in solutions I–V of the sample preparation protocol (Figure 1) when 19 mM Fos-10 is used in the NMR buffer. The OmpX concentration is given for the NMR sample volume of 50  $\mu\text{L}$ . (B) Relationship between Fos-10 concentrations in the NMR buffer and in the NMR sample (solution V in Figure 1). The solid line represents a linear regression. (C). Dependence of detergent concentration in the NMR sample (solution V in Figure 1) on the total amount of OmpX added to the sample. Measurements were performed with 19 mM and 31 mM Fos-10 concentration in the NMR buffer. The broken lines represent control experiments in which no protein was added to the solution. Each data point in panels B and C represents an OmpX reconstitution experiment with the protocol of Figure 1.

concentration devices, and the temperature during the concentration steps. The resulting concentrated protein solutions with known detergent content were then used to study the size and composition of the protein–detergent micelles at variable conditions.

**Preparation of Concentrated Membrane Protein Solutions with Defined Detergent Concentration.** In order to analyze the evolution of the detergent concentration during the reconstitution protocol (Figure 1), the Fos-10 concentration in the protein solution was determined by 1D  $^1\text{H}$  NMR spectroscopy (Figure 2), as described in the Materials and Methods section. Figure 3A shows the results for an experiment performed with 19 mM Fos-10 in the NMR buffer. Comparison of the concentration steps in I and II shows a small increase of detergent content in the sample, which we rationalize by the markedly different buffer compositions in solutions I and II. The amounts of Fos-10 at the end of steps II and V are similar, with only a slight trend toward lower concentrations arising from the fact that the NMR buffer contains lower amount of detergent than the

- (16) (a) Fernandez, C.; Adeishvili, K.; Wüthrich, K. *Proc. Natl. Acad. Sci. U.S.A.* **2001**, *98*, 2358–2363. (b) Fernandez, C.; Hilty, C.; Wider, G.; Wüthrich, K. *Proc. Natl. Acad. Sci. U.S.A.* **2002**, *99*, 13533–13537. (17) Lipfert, J.; Columbus, L.; Chu, V. B.; Lesley, S. A.; Doniach, S. *J. Phys. Chem. B* **2007**, *111*, 12427–12438. (18) Cantor, C. R.; Schimmel, P. R. *Biophysical Chemistry, Part 2*; Freeman: San Francisco, 1980. (19) (a) Strop, P.; Brunger, A. T. *Protein Sci.* **2005**, *14*, 2207–2211. (b) Maslennikov, I.; Kefala, G.; Johnson, C.; Riek, R.; Choe, S.; Kwiatkowski, W. *BMC Struct. Biol.* **2007**, *7*, 74.

**Table 1.** Fos-10 Up-concentration in the NMR Sample Observed for Different Centrifugal Devices and Different Temperatures for Sample Preparation<sup>a</sup>

device	temp. °C	MWCO <sup>b</sup>			
		10 kDa	30 kDa	50 kDa	100 kDa
Vivaspin polyethersulfone (PES)	4	5.5	4.2	3.6	1
Vivaspin polyethersulfone (PES)	25	4.9	3.2	1.5	1
Amicon (regenerated cellulose, C)	4	5.9	4.6	3.9	1

<sup>a</sup> The numbers in the table represent the ratio of the Fos-10 concentrations in the solution, *V* of Figure 1, and in the NMR buffer.  
<sup>b</sup> MWCO is the molecular weight cutoff of the centrifugal filter device.

refolding buffer (see Figure 1 and the Materials and Methods section for details). We then varied the detergent concentration in the NMR buffer and measured the resulting variation of detergent concentration in the NMR sample (Figure 3B). A linear relationship was thus found between the detergent concentrations in the NMR buffer and in the NMR sample, which provided a calibration curve for the preparation of OmpX/Fos-10 samples with specified detergent concentrations. In view of the pronounced up-concentration of the detergent in NMR sample *V*, when compared to the NMR buffer (Figure 1), we further investigated the impact of other experimental parameters on this process.

The effect of the total amount of protein present in the solution (some of which may not be properly reconstituted, depending on the detergent concentration) on the Fos-10 up-concentration was evaluated by two series of refolding experiments with Fos-10 concentrations in the NMR buffer of 19 and 31 mM. The amount of OmpX added to the sample was 0.0, 0.2, 1.0, and 1.7 mg. For both sets of experiments, the final detergent concentration of about 95 and 185 mM, respectively, was independent of the amount of OmpX added (Figure 3C).

Molecular weight cutoff (MWCO) and the type of centrifugal devices are known to largely affect the resulting detergent concentration.<sup>19</sup> Here, we compared Vivaspin polyethersulfone membranes (PES) and Amicon regenerated cellulose membranes (C) with MWCO values of 10, 30, 50, and 100 kDa (Table 1). The results show that the MWCO value plays an important role, whereas the type of membrane has only a negligibly small influence. Reduced detergent up-concentration at higher temperature was observed for all the tested concentration devices,<sup>20</sup> as illustrated in Table 1 for Vivaspin PES membranes. Larger MWCO values resulted in increased loss of protein from the concentrated solutions (I–V in Figure 1), both by absorption in the membrane and by flowthrough. For example, at 25 °C only about 70% and 50% of the protein were retained in solution I (Figure 1) when 50 kDa and 100 kDa MWCO were used, respectively. For the OmpX reconstitution we therefore used 10 kDa MWCO devices at 25 °C, which is a reasonable compromise regarding loss of OmpX, up-concentration of the detergent during the concentration steps, and duration of the sample preparation.

**Optimizing the NMR Spectra of OmpX/Fos-10 Micelles.** By use of samples of [<sup>2</sup>H,<sup>15</sup>N]-labeled OmpX reconstituted in mixed micelles with Fos-10 at defined detergent concentrations, the quality of the 2D [<sup>15</sup>N,<sup>1</sup>H]-TROSY correlation spectra of OmpX was evaluated for a wide range of detergent concentrations (Figure 4). The pattern of cross-peaks in these spectra was found

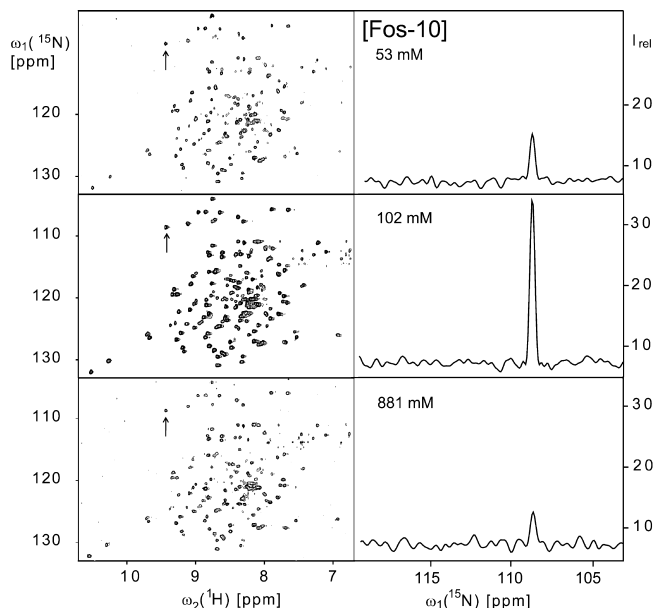


**Figure 4.** (Left-hand panels) Two-dimensional [<sup>15</sup>N,<sup>1</sup>H]-TROSY correlation NMR spectra of OmpX/Fos-10 mixed micelles at 53, 102, and 881 mM Fos-10 concentrations and 0.84, 1.04, and 0.77 mM [<sup>2</sup>H,<sup>15</sup>N]-OmpX concentrations in the NMR sample (solution *V* in Figure 1). The arrow points at the well-separated cross-peak of G143, for which the peak intensities, *I*<sub>rel</sub>, in the cross sections along ω<sub>1</sub>(<sup>15</sup>N) are shown in the corresponding right-hand panels. Identical acquisition and processing parameters were used to record the three data sets: data size 100 (*t*<sub>1</sub>) × 1024 (*t*<sub>2</sub>) complex points; *t*<sub>1max</sub> = 35.24 ms, *t*<sub>2max</sub> = 86.11 ms; 64 scans per *t*<sub>1</sub> increment, overall measurement time 4 h per experiment. Before Fourier transformation the data matrices were multiplied with an exponential window function in the acquisition dimension and with a 75°-shifted sine bell window<sup>22</sup> in the indirect dimension.

to be very similar for all the Fos-10 concentrations used, indicating that the conformation of the NMR-observable protein in these solutions is independent of the detergent content. In contrast, the cross-peak intensities depend strongly on the detergent content. A survey of six experiments of the type of Figure 4 shows that the average peak intensity, *I*<sub>rel</sub>, varies over nearly an order of magnitude among different detergent concentrations (Figure 5A). These differences in the signal intensities cannot be explained by variation of the protein concentration, which is closely similar in all the different samples (Figure 5A). While the NMR sensitivity at the lowest detergent concentration, 53 mM, indicates incomplete reconstitution of OmpX (see also text below), the signal variations at higher detergent concentrations called for additional investigations.

**Size and Composition of OmpX/Fos-10 Micelles from Studies of Rotational and Translational Diffusion.** The rotational diffusion coefficient, *D*<sub>r</sub>, was evaluated from the overall rotational correlation time, τ<sub>c</sub>, measured with the TRACT experiment (see Materials and Methods). The experimental *D*<sub>r</sub> values were found to depend linearly on the detergent concentration:

$$D_r = D_{r,0}(1 - \kappa_r C_{\text{Fos10}}) \quad (8)$$

where *D*<sub>r,0</sub> and κ<sub>r</sub> are fit parameters. A linear regression of the data gave *D*<sub>r,0</sub> and κ<sub>r</sub> values of 7.93 ± 0.20 × 10<sup>6</sup> s<sup>-1</sup> and 7.10 ± 0.03 × 10<sup>2</sup> M<sup>-1</sup>, respectively (Figure 5B), showing that the rotational tumbling of the mixed micelles slows down at high detergent concentrations. This variation of τ<sub>c</sub> with detergent concentration could be caused either by a change in the size of

(20) (a) Ericsson, C. A.; Soderman, O.; Garamus, V. M.; Bergstrom, M.; Ulvenlund, S. *Langmuir*. **2004**, *20*, 1401–1408. (b) Zulauf, M. *Crystallization of Membrane Proteins*; Michel, H., Ed.; CRC Press: Boca Raton, FL, 1991.

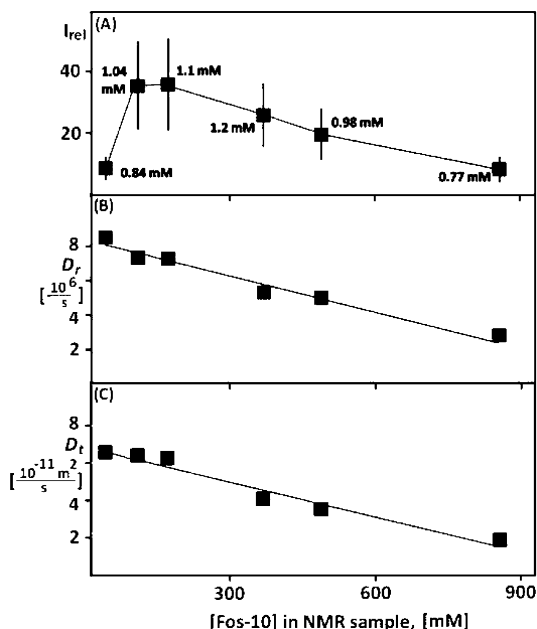


**Figure 5.** (A) Mean intensity of cross-peaks in the 2D [ $^{15}\text{N}$ , $^1\text{H}$ ]-TROSY correlation spectra of OmpX,  $I_{rel}$ , at variable Fos-10 concentrations in the NMR sample (solution V in Figure 1). The data at 53, 102, and 881 mM Fos-10 correspond to the spectra of Figure 4, left panels. The error bars represent the standard deviation from the mean taken over all the backbone  $^{15}\text{N}$ - $^1\text{H}$  cross peaks. For each data point the OmpX concentration is indicated, as determined by UV spectroscopy at 280 nm. (B) Rotational diffusion constant of OmpX,  $D_r$ , at variable Fos-10 concentrations, as determined by the TRACT NMR experiment.<sup>13</sup> (C) Translational diffusion coefficient,  $D_t$ , at variable Fos-10 concentrations as determined by the REST NMR experiment.<sup>14</sup> The data presented in panels A–C were recorded with the same OmpX/Fos-10 solutions. For further details on the NMR experiments used in panels B and C, see the Materials and Methods section.

the protein–detergent mixed micelles or by an increase of viscosity due to formation of empty micelles at high Fos-10 concentrations. To discriminate between these two possible explanations, we determined the dependence of the mixed-micelle hydrodynamic radii,  $R_h$ , on the detergent concentration by combining the information provided by the rotational and translational diffusion constants,  $D_r$  and  $D_t$ , respectively.  $D_t$  values for the same range of detergent concentrations as for  $D_r$  were determined by the REST experiment. We found that  $D_t$  depends linearly on the detergent concentration:

$$D_t = D_{t,0}(1 - \kappa_c c_{\text{Fos10}}) \quad (9)$$

with the following values for the two fit parameters:  $6.93 \pm 0.19 \times 10^{-11} \text{ m}^2 \text{ s}^{-1}$  for  $D_{t,0}$  and  $8.34 \pm 0.06 \times 10^2 \text{ M}^{-1}$  for  $\kappa_c$  (Figure 5C).

We then determined the value of the hydrodynamic radius  $R_h$  for each detergent concentration from the measured values of  $D_r$  and  $D_t$ , using eq 5, and compared them to the values for the radius of an equivalent sphere representing the micelles,  $R_m$ , calculated by use of different model assumptions on the influence of variable detergent concentrations on the size of mixed micelles (see Materials and Methods). A plot of the experimental  $R_h$  values versus the detergent concentration shows only a weak dependence, with a maximum of 26.0 Å at 102 mM Fos-10 and a minimum of 23.3 Å at 881 mM Fos-10. In contrast, a model in which all the detergent molecules that are not present as monomers in the solution would be incorporated into the mixed micelles predicts that the  $R_m$  value would increase from 25 Å at 102

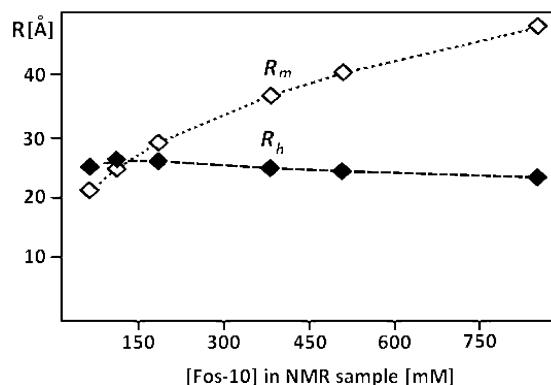


**Figure 6.** Dependence of the radius of an equivalent sphere representing the volume of the OmpX/Fos-10 mixed micelles on the Fos-10 concentration. ( $\diamond$ ) Results of a model calculation ( $R_m$ ) based on the assumptions that the OmpX concentration is 1 mM and detergent molecules are present exclusively either in mixed micelles with OmpX or as monomers (see Materials and Methods). ( $\blacklozenge$ ) Stokes radii,  $R_h$ , of the mixed micelles calculated with eq 5 from the translational and rotational diffusion coefficients  $D_t$  and  $D_r$  experimentally determined at an OmpX concentration of  $0.1 \pm 0.2 \text{ mM}$  (Figure 5). The broken lines connect points of the same data set, and are drawn to guide the eye.

mM Fos-10 to 47 Å at 881 mM Fos-10 (Figure 6). Since  $R_m$  values calculated with eq 7 represent a lower boundary of  $R_h$ , the results of Figure 6 indicate that the deterioration of the NMR spectrum at high detergent concentrations is not due to an increase of the size of mixed micelles. An increase in the viscosity of the solution due to excess detergent, which leads to concentrations far above the cmc and must therefore be present in the form of empty micelles, thus seems to be responsible for the decrease of  $D_t$  and  $D_r$ , and hence of  $I_{rel}$  (Figures 4 and 5A).

The linear dependence of  $D_t$  and  $D_r$  is in agreement with earlier theoretical and experimental studies, which report a linear concentration dependence of  $D_r$  in suspensions of particles with constant sizes and rationalize this behavior by the increased motional restrictions due to crowding effects at higher particle concentrations.<sup>21</sup> In this context, the fit parameters  $D_{t,0}$  and  $D_{r,0}$  can be interpreted as single-particle diffusion coefficients at infinite dilution that satisfy the Stokes–Einstein relationships of eqs 2–4, with the corresponding Stokes radius,  $R_{h,0}$ , and viscosity,  $\eta_0$ :

$$D_{t,0} = k_B T / (6\pi\eta_0 R_{h,0}) \quad (10)$$

$$D_{r,0} = k_B T / (8\pi\eta_0 R_{h,0}^3) \quad (11)$$

$$R_{h,0} = \sqrt{3D_{t,0}/4D_{r,0}} \quad (12)$$

The value of  $R_{h,0}$  for OmpX/Fos-10 mixed micelles is thus found to be  $25.9 \pm 0.3 \text{ Å}$ . The  $D_{r,0}$  value of  $7.93 \times 10^6 \text{ s}^{-1}$  corresponds to an effective rotational correlation time of 21 ns, which coincides closely with the experimental values of 21–25 ns, where  $\tau_c = 21 \text{ ns}$  was measured in samples with low detergent concentrations.<sup>13</sup> These values indicate that the OmpX/Fos-10 mixed micelles are approximately 50 kDa in size, with an aggregation number,  $N_a$ , of approximately 100 Fos-10 molecules per micelle.

(21) (a) Piazza, R.; Degiorgio, V.; Corti, M.; Stavans, J. *Phys. Rev. B* **1990**, *42*, 4885–4888. (b) Cichocki, B.; Ekiel-Jezewska, M. L.; Wajnryb, E. *J. Chem. Phys.* **1999**, *111*, 3265–3273. (c) Bernardo, P.; Garcia de la Torre, J.; Pons, M. *J. Mol. Recognit.* **2004**, *17*, 397–497.

(22) De Marco, A.; Wüthrich, K. *J. Magn. Reson.* **1976**, *24*, 201–204.

$R_{h,0}$  coincides closely with the  $R_m$  value calculated for 102 mM Fos-10 concentration (Figure 6), which is in the range where we obtained optimal NMR spectra (Figure 5A). Since the OmpX concentration in the NMR sample was 1.0 mM, we predict an aggregation number of approximately 90, which is based on the Fos-10 cmc of 10.8 mM and the assumption that the detergent molecules are either present as monomers in solution or incorporated into the mixed micelles. This prediction is in good agreement with the experimentally determined value of  $N_a = 100$ . These findings imply that for optimal sample conditions, the detergent molecules should either be bound to mixed micelles or monomeric in solution, so that the optimal Fos-10 concentration,  $c_{\text{Fos10}}^*$ , can be estimated by

$$c_{\text{Fos10}}^* = c_{\text{OmpX}} N_a + \text{cmc}_{\text{Fos10}} \quad (13)$$

For lower Fos-10 concentrations, the amount of detergent is too small to reconstitute all the OmpX molecules into mixed micelles so that some OmpX is not NMR-observable. This interpretation of our data at low detergent concentration (Figures 4, top left, and 5A) is in line with results from McDonnell and Opella.<sup>6</sup> Deterioration of the NMR spectra at high detergent content can be explained by an increase of viscosity due to excess detergent in the form of empty micelles, which slows down the diffusion of the protein—

detergent mixed micelles and thus causes line broadening and reduced signal intensity of the OmpX NMR spectra.

## Conclusions

The important conclusion from the present work for future studies with membrane proteins is the finding that high-quality NMR spectra can be obtained only over a very limited range of detergent concentrations. By use of our microcoil-NMR platform, this key result could be rationalized by investigations of the hydrodynamic properties of the IMP/detergent mixed micelles at discrete detergent concentrations in the NMR samples. The size of the OmpX/Fos-10 mixed micelles was thus found to be maintained at approximately 50 kDa over a large range of detergent concentrations. Deterioration of the NMR spectra at high detergent concentrations can be rationalized by a crowding effect due to formation of empty Fos-10 micelles, which slows down the molecular tumbling of the mixed micelles, resulting in faster spin relaxation.

**Acknowledgment.** This work was supported by the Joint Center for Innovative Membrane Protein Technologies (NIH Roadmap Grant P50 GM073197) and the Joint Center for Structural Genomics (NIH Grant U54 GM074898). K.W. is the Cecil H. and Ida M. Green Professor of Structural Biology at The Scripps Research Institute.

JA907842U